In situ Measurement of Young's Modulus of Carbon Nanotube inside TEM through Hybrid Nanorobotic Manipulation System

doi: 10.1109/TNANO.2006.874048

In Situ Measurement of Young's Modulus of Carbon Nanotubes Inside a TEM Through a Hybrid Nanorobotic Manipulation System

Masahiro Nakajima, *Student Member, IEEE*, Fumihito Arai, *Member, IEEE*, and Toshio Fukuda, *Fellow, IEEE*

***Abstract*—A hybrid nanorobotic manipulation system inside a scanning electron microscope (SEM) and a transmission electron microscope (TEM) is presented. The SEM manipulators have been constructed with 8 degrees of freedom (DOFs) with three units for effective TEM sample preparation. The TEM manipulator consists of a 3-DOF manipulator actuated with four multilayer piezoelectric actuators and a 3-DOF passively driven sample stage. High resolution and transmission image of TEM is readily used for measurement and evaluation of samples. The stage is premanipulated by the SEM manipulator for sample preparations inside the SEM. This methodology is called the hybrid nanorobotic manipulation so as to differentiate it from those with only an exchangeable specimen holder. To show the effectiveness of the system, the Young's modulus of a carbon nanotube (CNT) was measured to be 1.23 TPa inside a TEM after being premanipulated inside the SEM. With this system, we can measure the inner diameter of a CNT and improve the accuracy in measuring the Young's modulus of a CNT.**

***Index Terms*—Carbon nanotubes (CNTs), electron microscope, nanorobotic manipulation, nanotechnology, Young's modulus.**

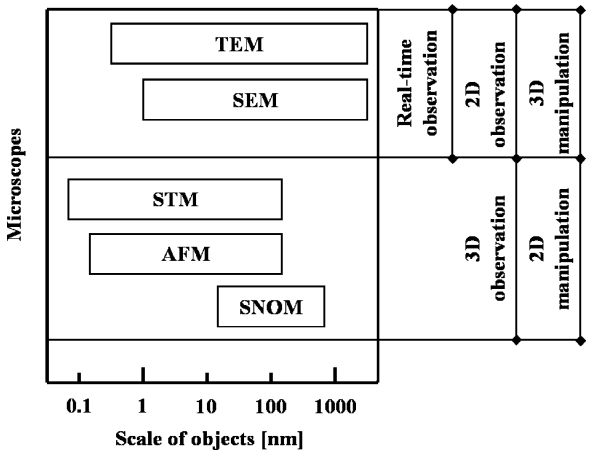

Fig. 1. Strategies of nanomanipulation with microscopes.

I. Introduction

NANOMANIPULATION has received much more attention than ever, because it is an effective strategy for the property characterizations of individual nanoscale objects and the construction of nanoscale devices to realize high-integration, multifunction, low-energy consumption, and so on. To manipulate nanoscale objects, they must be observed with a resolution higher than nanoscale. Hence, a manipulation system and an observation system, e.g., a microscope in general, are necessary for nanomanipulations.

Scanning probe microscopes (SPMs), such as scanning tunneling microscopes (STMs) or atomic force microscopes (AFMs), have functions of both observation and manipulation. The feasibility has been shown by the first practice on nanomanipulation demonstrated by Eigler and Schweizer. An STM is applied for positioning individual Xe atoms on a nickel surface with atomic precision at low temperature [1]. Hertel *et al.* applied an AFM to bend and translate carbon nanotubes (CNTs) on a substrate [2]. Their high resolution makes them capable of atomic manipulation; however, their observation space is too narrow and constrained in a plane.

Electron microscopes, such as scanning electron microscopes (SEMs) and transmission electron microscopes (TEMs), show their uniqueness in the capability to contain an independent manipulator inside the specimen chamber for three-dimensional (3-D) manipulation. High resolution and transmission images of TEMs are useful for the measurement and evaluation of nanoscale objects. Some groups have demonstrated manipulations using a piezotube-driven nanomanipulator inside the specimen holder: Kizuka *et al.* constructed a manipulator inside a high-resolution TEM (HRTEM) to investigate atomic scale contact and noncontact scanning on gold surfaces [3]. Cumings and Zettl demonstrated a sliding motion between different layers of multiwalled CNTs (MWCNTs) inside a TEM [4]. However, the specimen chamber and observation area of the TEM are too narrow to contain manipulators with complex functions. Special sample preparation techniques are also needed.

Our previous works have shown a nanorobotic manipulator constructed inside a field-emission SEM (FE-SEM) that can be applied for quite complex nanomanipulations [6]–[8]. However, the resolution of an SEM is generally one order of magnitude lower than that of a TEM. Fig. 1 shows the strategies of nanomanipulations with different kinds of microscopes [8]. Before an ideal microscope can be invented, it is a practical strategy to combine different microscopes so as to take both the resolution and complexities into account

Manuscript received April 15, 2005; revised November 22, 2005. This work was supported in part by the Ministry of Education, Science, Sports, and Culture Grant-in-Aid for Scientific Research under Contract 15360136. The review of this paper was arranged by Associate Editor B. Nelson.

The authors are with the Department of Micro–Nano Systems Engineering, Nagoya University, Nagoya City 464-8603, Japan (e-mail: nakajima@robo.mein.nagoya-u.ac.jp; arai@mein.nagoya-u.ac.jp; fukuda@mein.nagoya-u.ac.jp).

Digital Object Identifier 10.1109/TNANO.2006.874048

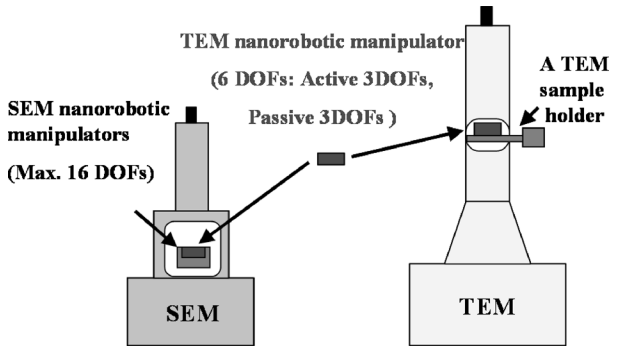

Fig. 2. Configuration of a hybrid nanorobotic manipulation system.

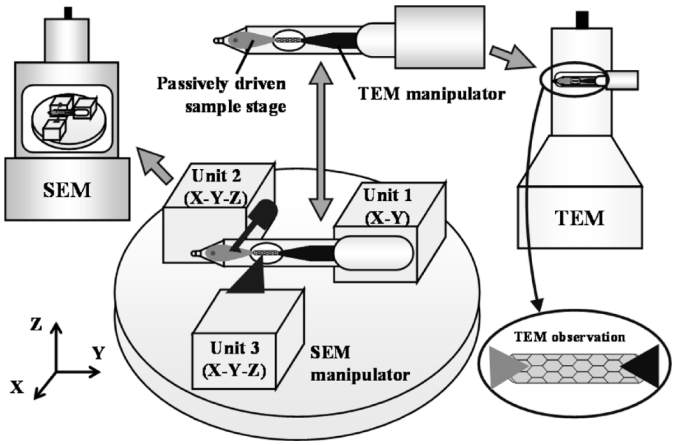

Fig. 3. Schematic diagram of the hybrid nanorobotic manipulation system.

In this paper, we propose an exchangeable manipulator between an FE-SEM and a TEM [9], [10]. The configuration is as shown in Fig. 2. The strategy is called hybrid manipulation so as to differentiate it from those with only an exchangeable specimen holder. The most important feature is that it contains several passive degrees of freedom (DOFs), which makes it possible to perform relatively complex manipulations while a compact volume can be installed inside the narrow vacuum chamber of a TEM.

II. Hybrid Nanorobotic Manipulation System

The hybrid nanorobotic manipulation system integrates a TEM nanorobotic manipulator (TEM manipulator) into an SEM nanorobotic manipulator (SEM manipulator). Fig. 3 shows the schematic diagram of the hybrid nanorobotic manipulations system. The TEM manipulator can be set inside an SEM and a TEM for sample preparation. It is also mounted a passively driven sample stage. The stage is premanipulated by the SEM manipulator for sample preparations inside the SEM. The methodology is named the hybrid nanorobotic manipulation so as to differentiate it from those with only an exchangeable specimen holder. This system can realize an efficient sample preparation with a sufficiently wide working space of SEM manipulators and sufficiently high resolution to identify nanoscale objects with a TEM.

In this paper, an FE-SEM (JEOL, JSM-6500F) and a TEM (Hitachi, H-800) are used. Their specifications are listed in Table I. The resolution of H-800 is ten times higher than that of JSM-6500F; it is of subnano order. On the other hand, the observation space of JSM-6500F is approximately 10 000 times larger than that of H-800. Hence, TEM is well suited to measure and evaluate nanoscale objects, and SEM is preferred for setting manipulators and samples for efficient sample preparation.

TABLE I
Specifications of FE-SEM (JSM-6500F) and TEM (H-800)

Electron Microscope	TEM (Hitachi, H-800)	FE-SEM (JEOL, JSM-6500F)
Acceleration Voltage	35 ~ 200 kV	0.5 ~ 30 kV
Magnification	×1,000 ~ ×600,000	×10 ~ ×500,000
Resolution	0.24 nm (lattice interval) ,0.45 nm (point-point interval)	1.5 nm
Observation Space	ϕ2 mm × ± 0.3 mm	70 mm × 50 mm × 3~40 mm

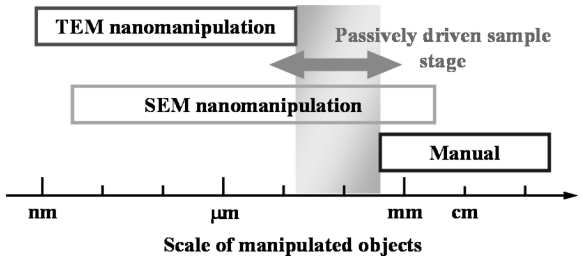

Fig. 4. Scale of manipulated objects through TEM and SEM manipulations.

A. Passively Driven TEM Sample Stage

The space of a TEM sample chamber is quite narrow and strictly limited due to the principle of a TEM, which includes a high vacuum environment, short distance between an upper and a lower polepiece, short working distance, and so on. These space limitations cause the difficulty of constructing multi-DOF manipulation systems inside a TEM sample chamber. Fig. 4 shows the scale of manipulated objects through SEM and TEM manipulations. The working space of a TEM manipulator is also much smaller than that of an SEM manipulator with normally used actuators. If the actuation mechanism is installed in the outside of a sample chamber, it has a high cost and is limited at the reconstruction of a TEM. On the other hand, manual adjustment can be reached only $\sim 100\ \mu$m from the positioning resolution of a sample. Hence, it is difficult to adjust the position of a sample within the working area of the TEM manipulator manually. Here, we propose a sample stage passively driven by SEM nanorobotic manipulators for coarse positioning adjustment of TEM samples. Classification of the passive driven mechanism is given here and shown in Fig. 5: (a) friction type, (b) screw type, (c) plastic deformation type, (d) elastic deformation type, (e) electrostatic type, and (f) magnetic force type. Types (a)–(c) are relatively easy to be constructed and used as disposable. Types (d)–(f) have relatively high endurance; however, their complex mechanisms are not easy to be constructed

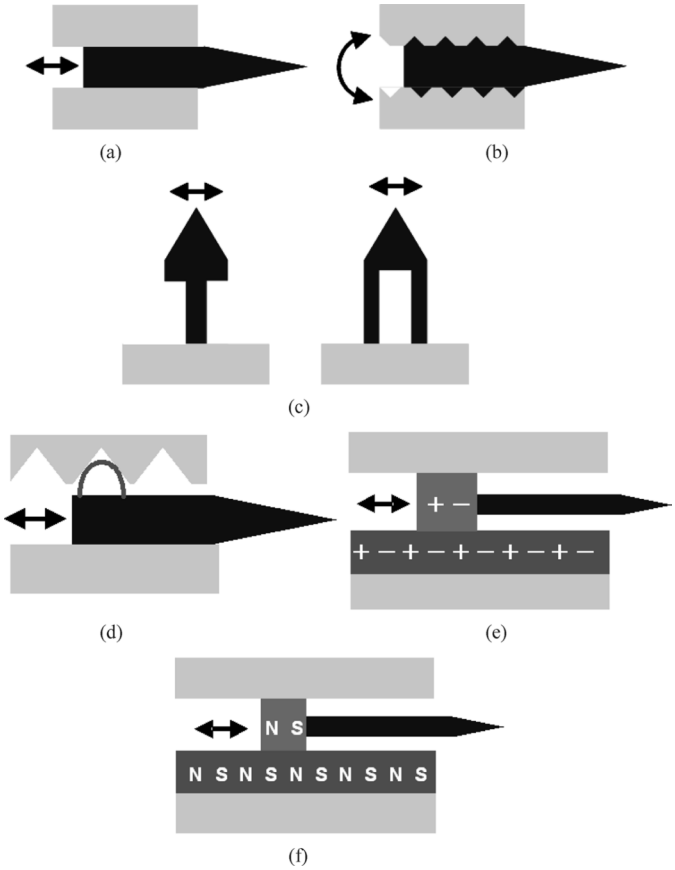

Fig. 5. Positioning mechanisms of passive sample stage. (a) Friction type. (b) Screw type. (c) Plastic deformation type. (d) Elastic deformation type. (e) Electrostatic force type. (f) Magnetic force type.

with a sufficiently high positioning resolution. In this paper, type (c) is applied for the mechanism of the passively driven stage. The hinge beams of a TEM sample stage are plastically deformed by the SEM manipulator to be set within the working area of the TEM manipulator.

Fig. 6 shows the schematic diagram of a constructed passively driven sample stage. Samples are fixed at the tip of the sample stage. The sample stage has two holes; one is used for driving by SEM manipulators and the other is used for fixation on a TEM sample holder. The two thin beams and a plate are driven in the X-, Y-, and Z-directions, for the X-direction by bent of two beams [see Fig. 6(b)], for the Y-direction by tensile and compressive bent of two beams [see Fig. 6(b)], and for the Z-directions by twist bent of a plate and beams [see Fig. 6(c)]. Fig. 7 shows the configuration of a passively driven sample stage and an end-effecter of the SEM manipulator.

To avoid the magnetic field produced by processing, a nonmagnetic metal is needed. We have always used aluminum [9], [10]; however, a relatively large elastic deformation is not suitable for precise operation, and this causes the error of the stage movement at plastic deformation. In this paper, indium and lead are used as the low-strength material. Fig. 8 shows the plastic deformation of an indium passively driven sample stage at each movement. On the average of ten $\sim$ 20-μm movements, the positioning resolutions are $\sim$ 12 μm in the X-direction (positioning error: $\sim$ 6 μm), and $\sim$ 15 μm in the Y-direction (positioning error: $\sim$ 5 μm). These values are $\sim$5 and $\sim$2 times

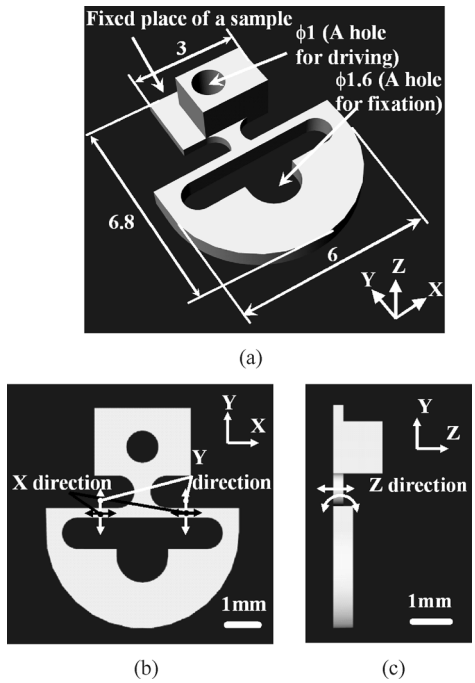

Fig. 6. Schematic diagram of a passively driven sample stage. (a) 3-D view. (b) Top view. (c) Side view.

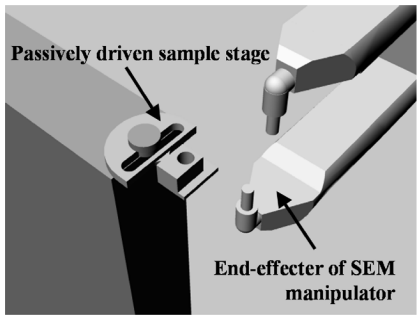

Fig. 7. Schematic diagram of a passively driven sample stage and an end-effecter of the SEM manipulator.

higher positioning resolution and $\sim$14 and $\sim$3% low positioning error compared with the aluminum stage.

B. TEM Nanorobotic Manipulation System

Fig. 9 shows the 3-D schematic diagram of the TEM nanomanipulator. It consists of four multilayer piezoelectric devices, two two-hinge beams, a plate for sample fixation, and a base. All parts are made of aluminum to avoid the magnetic field produced by processing. The two hinge beams are used for the translational movements in the X- and Z-directions, as shown in Fig. 9(b) and (c).

Fig. 10 shows the overview of the constructed TEM nanomanipulator. The TEM manipulator can be installed inside a normal-type side-entry TEM sample holder, which has an inner diameter of 7 mm, as shown in Fig. 11. It is set on the side-entry-type TEM sample holder, as shown in Fig. 12. The tip part is able to be removed for setting on the SEM manipulator. The specifications of the TEM manipulator are listed in Table II.

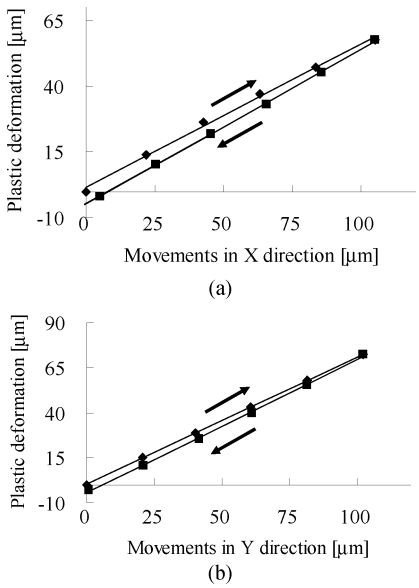

Fig. 8. Plastic deformation of the passively driven sample stage. (a) X-direction. (b) Y-direction.

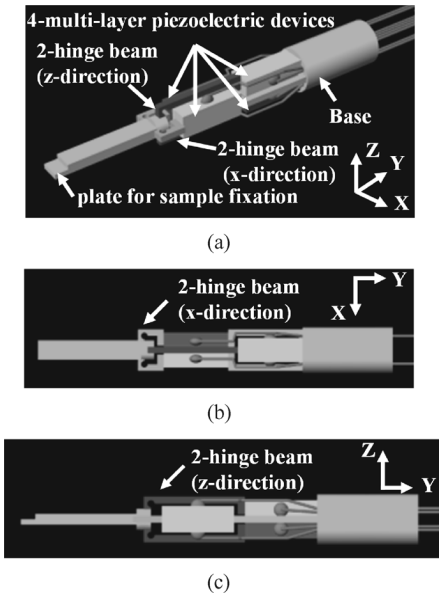

Fig. 9. 3-D schematic diagram of a TEM nanorobotic manipulator. (a) Overview. (b) Top view. (c) Side view.

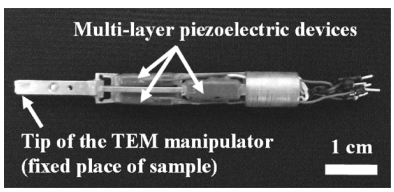

Fig. 10. TEM nanorobotic manipulator (top view).

C. SEM Nanorobotic Manipulation System

The SEM manipulators have been constructed with a maximum of 16 DOF with four units [6]–[8]. The characteristics of SEM manipulators include a sufficiently wide working space and multiprobes with multiunits for preparing samples. In this paper, SEM manipulators are reconstructed to be 8 DOF with three units for integration of the TEM manipulator. The overview of SEM manipulator is shown in Fig. 13. A gas introduction system is equipped on the SEM, and it can be readily used for nanofabrication.

Unit 1 is used for driving the TEM manipulator and the fixation of samples. Unit 2 is used for driving the passive sample

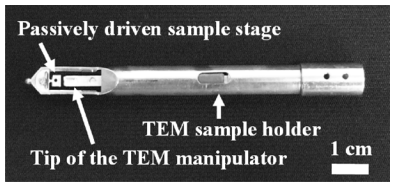

Fig. 11. TEM manipulator inserted inside a TEM sample holder.

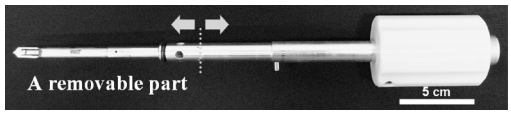

Fig. 12. TEM sample holder installed the TEM manipulator.

TABLE II
SPECIFICATIONS OF A HYBRID NANOROBOTIC MANIPULATION SYSTEM

Items	Specifications
TEM Nanorobotic Manipulator (Fig. 7~10)	
DOFs	3 DOFs (X, Y, Z), Passive 3 DOFs (X, Y, Z)
Actuators	4 multi-layer piezoelectric devices
Working Space	~ 8 μm × ~ 60 μm × ~ 60 μm
SEM Nanorobotic Manipulator (Fig. 11)	
DOFs	Unit1: 2 DOFs (X, Y), Unit2: 3 DOFs (X, Y, Z), Unit3: 3 DOFs (X, Y, Z), Total: 8 DOFs
Actuators	6 Picomotors™, (Unit1, Unit2,Uni3-Z) 2 Nanomotors™ (Unit3-X,Y)
Working Space	~ 16 mm × ~ 16 mm × ~12 mm
Positioning Resolution	~ 30 nm (Unit 1: X, Y, Unit2: X, Y, Z, Unit3: Z), ~2nm (Unit3: X, Y)
SEM Nanofabrication System	
EBID	FE-SEM emitter, CNT emitter, Gas introduction system

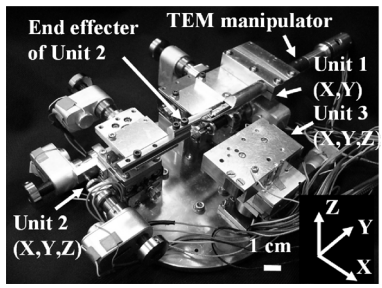

Fig. 13. SEM nanorobotic manipulators.

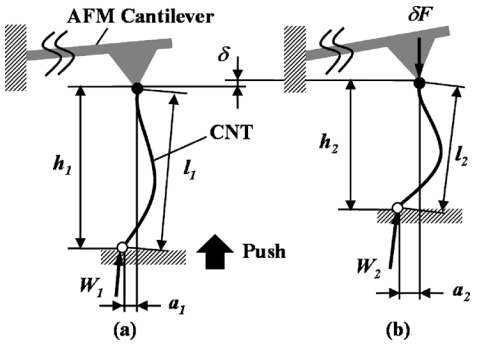

Fig. 14. Schematic diagram of a buckled CNT for measurement of its bending modulus.

stage of the TEM manipulator, which will be described in Section II-A. Unit 3 is used for the fixation of samples. The specifications of the SEM manipulators are listed in Table II.

III. *In Situ* Measurement of Young's Modulus of a CNT Inside the TEM

To demonstrate the effectiveness of the hybrid nanorobotic manipulation system, the elasticity of an MWCNT is measured inside a TEM with *in situ* force measurement using an AFM cantilever.

A. Model of Measurement of Young's Modulus of a Nanotube by the Buckling Process

Fig. 14 shows the analytic model for the measurement of the elastic modulus of a CNT by the buckling process. Fig. 14(a) and (b) shows the continuous buckling process of a CNT. Assuming that the CNT is a continuous model, from Euler's formula and force balance relations, the following equations can be obtained:

$$\begin{cases} W_1 = \frac{\pi^2 E_{\mathrm{CNT}} I_{\mathrm{CNT}}}{(cl_1)^2}, W_2 = \frac{\pi^2 E_{\mathrm{CNT}} I_{\mathrm{CNT}}}{(cl_2)^2} \\ \delta F = k\delta \\ \delta F = \frac{h_2}{(cl_2)} W_2 - \frac{h_1}{(cl_1)} W_1 \end{cases} \tag{1}$$

where W_1 and W_2 are the buckling forces applied to a CNT, δF is the difference of reaction force by an AFM cantilever, k is the spring constant of an AFM cantilever, E_{CNT} is the Young's modulus of a CNT, l_1 and l_2 are the distance between two ends of the buckled CNT, and I_{CNT} is the geometrical moment of inertia of a CNT. In this equation, l_1 and l_2 are corrected by the multiplication of c: 0.8, which is recommend by the Structural Stability Research Council (SSRC) [11]. From these equations, the Young's modulus of a CNT E_{CNT} is as follows:

$$E_{\mathrm{CNT}} = \frac{64k\delta}{(d_{\mathrm{oCNT}}^4 - d_{\mathrm{iCNT}}^4)\pi^3 \left(\frac{h_2}{(cl_2)^3} - \frac{h_1}{(cl_1)^3}\right)} \tag{2}$$

where d_{oCNT} and d_{iCNT} are the outer and inner diameters of a CNT. The values of a_1, a_2, h_1, h_2, δ, d_{oCNT}, and d_{iCNT} are measured from TEM images, l_1 and l_2 are calculated values from $l_1 = \sqrt{a_1^2 + h_1^2}$, and $l_2 = \sqrt{a_2^2 + h_2^2}$.

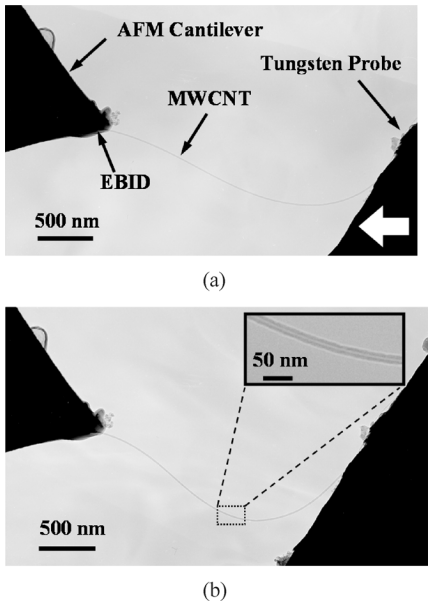

Fig. 15. Sequential TEM photographs during buckling of a MWCNT. (a) Before pushing. (b) After pushing.

B. In Situ Measurement of Young's Modulus of a CNT Inside a TEM

In this experiment, MWCNTs synthesized by the arc discharge method are used [12]. First, a CNT is picked up on an AFM cantilever (Olympus OMCL-TR400PB, k: 0.03 N/m) from bulk samples through electron-beam-induced deposition (EBID) [13]. The AFM cantilever is set on a passive sample stage and it is positioned within the working area of the TEM manipulator, as presented in Section II-A.

Fig. 15 shows two sequential TEM photographs during the buckling of an MWCNT (d_{oCNT}: 14.3 nm, d_{iCNT}: 3.2 nm). One end of a CNT is fixed on an AFM cantilever by EBID inside a SEM the other end is adhered on a tungsten needle probe by van der Waals forces. From these images, the parameters are measured as a_1: 0.447 μm, a_2: 0.318 μm, h_1: 2.36 μm, h_2: 2.10 μm, and δ: 84.0 nm. The values of l_1 and l_2 are calculated as 2.41 and 2.12 μm. Hence, the elastic modulus of this CNT E_{CNT} is calculated to be $1.23\ ^{+0.09}_{-0.08}$ TPa. This value is same order with ~ 1 TPa from theoretical analysis [14] and experimental results [15]. Comparing with the *in situ* SEM measurement at same experimental parameters (maximum image resolution: 1.5 nm, JSM-6500F), $-33.1\% \sim +58.2\%$ relative error is caused by the measurement error on the diameter of a CNT. It is not possible to measure the inner diameter of a CNT by SEM, hence 0.2% relative error is caused d_{iCNT}: 0 on (2). From the *in situ* measurement inside a TEM, we can measure the inner diameter of a CNT and improve the accuracy in measuring the Young's modulus of a CNT.

IV. Conclusion

A hybrid nanorobotic manipulation system, which is integrated into a nanorobotic manipulator inside a TEM and an SEM, has been proposed. The TEM nanomanipulator was constructed with a 3-DOF unit activated with four multilayer

piezoelectric devices and a passive sample stage driven by SEM nanorobotic manipulators. The system is realized with a sufficiently wide working space through the SEM nanomanipulator and a sufficiently high resolution with a TEM for identification of nanoscale objects with efficient and complex nanomanipulations. To demonstrate the effectiveness of the system, the elasticity of a CNT was measured to be 1.23 TPa inside a TEM after premanipulation inside a SEM.

ACKNOWLEDGMENT

The authors are grateful to Prof. Y. Saito at Nagoya University for providing the MWCNTs and S. Arai at Nagoya University for help with the operation of the TEM.

REFERENCES

[1] D. M. Eigler and E. K. Schweizer, "Positioning single atoms with a scanning electron microscope," *Nature*, vol. 344, pp. 524–526, 1990.
[2] T. Hertel, R. Martel, and P. Avouris, "Manipulation of individual carbon nanotubes and their interaction with surfaces," *J. Phys. Chem. B*, vol. 102, no. 6, pp. 910–915, 1998.
[3] T. Kizuka, K. Yamada, S. Deguchi, M. Naruse, and N. Tanaka, "Cross-sectional time resolved high-resolution transmission electron microscopy of atomic-scale contact and noncontact-type scannings on gold surfaces," *Phys. Rev. B, Condens. Matter*, vol. 55, no. 12, pp. 7398–7401, 1997.
[4] Z. L. Wang, Z. R. Dai, R. Gao, and J. L. Gole, "Measuring the Young's modulus of solid nanowires by in situ TEM," *J. Electron. Microscopy*, vol. 5, no. 2, pp. S79–85, 2002.
[5] J. Cumings and A. Zettl, "Low-friction nanoscale linear bearing realized from multiwall carbon nanotubes," *Science*, vol. 289, pp. 602–604, 2000.
[6] L. X. Dong, F. Arai, and T. Fukuda, "Destructive constructions of nanostructures with carbon nanotubes through nanorobotic manipulation," *IEEE/ASME Trans. Mechatronics*, vol. 9, no. 2, pp. 350–357, 2004.
[7] M. Nakajima, F. Arai, L. X. Dong, and T. Fukuda, "Calibration of carbon nanotube probes for pico-Newton order force measurement inside a scanning electron microscope," *J. Robot. Mechatron.*, vol. 16, no. 2, pp. 155–162, 2004.
[8] T. Fukuda, F. Arai, and L. X. Dong, "Assembly of nanodevices with carbon nanotubes through nanorobotic manipulations," *Proc. IEEE*, vol. 91, no. 11, pp. 1803–1818, Nov. 2003.
[9] M. Nakajima, F. Arai, L. X. Dong, and T. Fukuda, "A hybrid nanorobotic manipulation system inside scanning and transmission electron microscope," in *Proc. 4th IEEE Conf. Nanotechnol.*, 2004, TU_P35, pp. 462–466.
[10] ——, "Hybrid nanorobotic manipulation system inside scanning electron microscope and transmission electron microscope," in *Proc. IEEE/RSJ Int. Conf. Intell. Robots Syst.*, 2004, pp. 589–594.
[11] B. G. Johnston, *Guide to Stability Design Criteria for Metal Structures*. New York: Wiley, 1976, pp. 64–74.
[12] Y. Saito, T. Yoshikawa, and M. Inagaki, "Growth and structure of graphitic tubules and polyhedral particles in arc-discharge," *Chem. Phys. Lett.*, vol. 204, no. 3, 4, pp. 277–282, 1993.
[13] L. X. Dong, F. Arai, and T. Fukuda, "Electron-beam-induced deposition with carbon nanotube emitters," *Appl. Phys. Lett.*, vol. 81, no. 10, pp. 1919–1921, 2002.
[14] J. P. Lu, "Elastic properties of carbon nanotubes and nanoropes," *Phys. Rev. Lett.*, vol. 79, no. 7, pp. 1297–1300, 1997.
[15] E. W. Wong, P. E. Sheehan, and C. M. Lieber, "Nanobeam mechanics: Elasticity, strength, and toughness of nanorods and nanotubes," *Science*, vol. 277, pp. 1971–1975, 1997.

Masahiro Nakajima (S'03) received the B.S. degree from Shizuoka University, Shizuoka, Japan, in 2001, the M.S.Eng. degree from Nagoya University, Nagoya, Japan, in 2003, and is currently working toward the Ph.D. degree in micro system engineering at Nagoya University.

His research interests include applications of nanorobotic manipulation, nanodevices, and nanomechanics.

Fumihito Arai (M'91) received the B.S. and M.S. degrees from the Science University of Tokyo, Tokyo, Japan, in 1986 and 1988, respectively, and the Dr.Eng. degree from Nagoya University, Nagoya, Japan, in 1993.

From 1988 to 1989, he was Research Fellow with the Fuji Photo Film Company Ltd., Japan. He joined Nagoya University in 1989 as Research Associate. Since 1998, he has been an Associate Professor with the Department of Micro System Engineering, Nagoya University, where he has mainly been involved in the research fields of micro/nano robotics and the application to the micro/nano-assembly and bio automation, bio-MEMS, bio-chips, medical robotics, microsensors and microactuators, carbon nanotube and nano devices, intelligent robotic systems, and intelligent human–machine interface.

Toshio Fukuda (M'83–SM'93–F'95) received the B.S. degree from Waseda University, Tokyo, Japan, in 1971, and the M.S. and Dr.Eng. degrees from the University of Tokyo, Tokyo, Japan, in 1973 and 1977, respectively.

From 1977 to 1982, he was with the National Mechanical Engineering Laboratory, Tsukuba, Japan. From 1982 to 1989, he was with the Science University of Tokyo, Tokyo, Japan. Since 1989, he has been with Nagoya University, Nagoya, Japan, where he is currently a Professor with the Department of Micro–Nano Systems Engineering, where he has mainly been involved in the research fields of intelligent robotic systems, cellular robotic systems, mechatronics, and micro- nanorobotics.

Dr. Fukuda was the President of the IEEE Robotics and Automation Society (1998–1999), the Director of the IEEE Division X, Systems and Control (2001–2001), and the Editor-in-Chief of the IEEE/ASME TRANSACTIONS ON MECHATRONICS (2000–2002). He is currently the President of the IEEE Nanotechnology Council.